Received: 1 January 2021 | Revised: 20 September 2021 | Accepted: 22 September 2021

DOI: 10.1002/eng2.12468

RESEARCH ARTICLE

Engineering Reports Open Access WILEY

An electronic textile embedded smart cementitious composite

Muhammad S. Irfan[1] | **Muhammad A. Ali**[1] | **Kamran A. Khan**[1] | **Rehan Umer**[1] | **Antonios Kanellopoulos**[2] | **Yarjan Abdul Samad**[3]

[1]Department of Aerospace Engineering, Khalifa University of Science and Technology, Abu Dhabi, United Arab Emirates

[2]Centre for Engineering Research, School of Engineering & Computer Science, University of Hertfordshire, Hatfield, UK

[3]Cambridge Graphene Centre, Engineering Department, University of Cambridge, Cambridge, UK

Correspondence
Yarjan Abdul Samad, Cambridge Graphene Centre, Engineering Department, University of Cambridge, 9, JJ Thomson Avenue, Cambridge CB3 0FA, UK.
Email: yy418@cam.ac.uk
Kamran A. Khan, Department of Aerospace Engineering, Khalifa University of Science and Technology, Abu Dhabi, United Arab Emirates.
Email: kamran.khan@ku.ac.ae

Funding information
Abu Dhabi Award for Research Excellence, Grant/Award Number: 8434000349; Khalifa University of Science, Technology and Research, Grant/Award Numbers: 8474000195, Internal grants CIRA-2018-15 and FSU-2019-08

Abstract

Structural health monitoring (SHM) using self-sensing cement-based materials has been reported before, where nano-fillers have been incorporated in cementitious matrices as functional sensing elements. A percolation threshold is always required in order for conductive nano-fillers modified concrete to be useful for SHM. Nonetheless, the best pressure/strain sensitivity results achieved for any self-sensing cementitious matrix are $<0.01\,MPa^{-1}$. In this work, we introduce for the first-time novel partially reduced graphene oxide based electronic textile (e-textile) embedded in plain and as well as in polymer-binder-modified cementitious matrix for SHM applications. These e-textile embedded cementitious composites are independent of any percolation threshold due to the interconnected fabric inside the host matrix. The piezo-resistive response was measured by applying direct and cyclic compressive loads (ranging from 0.10 to 3.90 MPa). A pressure sensitivity of $1.50\,MPa^{-1}$ and an ultra-high gauge factor of 2000 was obtained for the system of the self-sensing cementitious structure with embedded e-textiles. The sensitivity of this new system with embedded e-textile is an order of magnitude higher than the state-of-the-art nanoparticle based self-sensing cementitious composites. The composites showed mechanical stability and functional durability over long-term cyclic compression tests of 1000 cycles. Additionally, a two time-constant model was used to validate the experimental results on decay response of the e-textile embedded composites.

KEYWORDS

2D materials, cementitious composites, in situ sensors, piezoresistivity, polymer composites, strain sensors

JEL CLASSIFICATION

Materials science

1 | INTRODUCTION

Civil infrastructure (dams, bridges, tunnels, road network etc.) plays a vital role in our societal and economic growth. Concrete and the related cement-based materials are the construction industry's favorites for a variety of reasons: (i) ease and cost of construction compared to alternatives (e.g., steel); (ii) robustness for a variety of exposure scenarios; (iii) ability to construct a large variety of complex geometries and (iv) excellent mechanical performance.[1] These materials have excellent response in compressive loads and typically display quasi-brittle behavior. To be used for infrastructure projects the presence of steel reinforcement is essential. Steel alleviates the quasi-brittle behavior of concrete and the new composite (reinforced concrete) can sustain well both compressive and flexural loads. The exposure of cement-based infrastructure to a vast number of degrading environments throughout their service life cannot be prevented. The integrity of concrete and cement related materials largely depend on their ability to withstand mechanical and environmental weathering. It is the coupled effect of phenomena such as impact, service loading, chloride/CO_2 concentration, pressure/thermal differentials, freeze–thaw, and sulfates that can cause severe damage, hence reducing functionality.[2] Damage can manifest itself by localized weakening of the material and can progress in the form of microcracks that gradually reduce the integrity of structures and elements. Under continuous mechanical and environmental stress these microdefects coalesce and expand thus compromising the mechanical properties of materials. In order to monitor the in-service integrity of the cement-based structures, structural health monitoring (SHM) is deemed vital especially for the safety of the critical components.[3] SHM can provide real-time data about the condition of a structure by using suitable sensors. This will allow for timely intervention in critical situations minimizing considerably the maintenance regimes and extending the service life of an infrastructure asset. Conventionally, these sensors are either embedded or applied on the external surfaces of the structure.[4] A number of sensing techniques including, foil strain gauge,[5] optical fiber,[5,6] piezoelectric ceramic,[7,8] and shape memory alloys[7] have been studied for SHM of cement-based constructions. A comparison of different structure heath monitoring (SHM) techniques used in concrete and cement structures is provided by Dong et al. in their review.[9] Such sensors are usually incompatible with cementitious materials and reduce the strength and durability of the structure.[10] Recently some work has been reported on the technologies involving SHM and Internet of Things (IoT).[11,12] The basic principle here is to acquire the real-time data from the sensors by integration of radio frequency identification (RFID) tag antennas, wireless sensors network (WSN), and sensors.

A lot of work has been reported on self-sensing cement-based materials based on fillers like carbon fibers (CFs),[13–15] carbon nanotubes (CNTs),[1,13,16,17] hexagonal boron nitride (hBN),[18] graphene oxide (GO),[18–25] carbon nanofibers (CNFs),[26] graphite nanofibers (GNFs),[10] graphene nanoplatelets (GNPs),[27,28] carbon black,[29–31] steel fibers,[32–34] nickel powders,[35,36] conductive rubber,[37,38] and MXenes.[39] A major challenge in using these fillers is their homogeneous dispersion in the cementitious matrix especially in large volumes.[40] Most of the reported work involves modification of the cementitious matrix at nanoscale and shows improvement or retention of mechanical properties while providing the self-sensing capabilities via piezo-resistive response. Nonetheless, the application of these fillers at large volumes is a technical and economic challenge. After we introduced RGO coated electronic textiles in early 2014[41] instead of using nanofillers in the bulk material, some researchers have employed such smart textiles as sensor elements in the field of fiber reinforced composites to monitor the processing parameters and in-service strain.[42–44] Recently, we have developed a simple and scalable application of pRGO coated substrates for pressure sensing.[45] The method has been applied to wearable items for real-time health and physical performance monitoring. All the applications have demonstrated both repeatability and scalability.

Various polymers such as urea-formaldehyde resin, unsaturated polyester resin, methylmethacrylate, epoxy resin, furan resins, polyurethane resins, and waste tire rubber have been used by researchers to create polymer-modified mortar (PMM)/polymer-modified concrete (PMC).[46–50] There are two major reasons for adding polymeric materials to the cementitious matrix: (i) to re-use the waste polymer; and (ii) to change specific properties of the cement-based materials for example, density, fatigue life, toughness, brittleness, and moisture absorbance.[47] The effect of polymer modification on the piezo-resistivity of self-sensing cement-based composites has not been reported.

In this work, we present the application of partially reduced graphene oxide (pRGO)-coated Nylon® textile as the piezo-resistive strain-sensing element in a cement-based system. A comparison was also made between matrices with and without polymer modification. It was shown that the pRGO-coated piezo-resistive fabric provides a novel route for

making self-sensing cement-based materials and the addition of polymer in the matrix improves the sensing and bonding capabilities of the structure to a great extent.

2 | MATERIALS AND METHODS

2.1 | Preparation of pRGO coated Nylon® fabric

The e-textile was prepared by coating graphene oxide (GO) on a commercially available Nylon® fabric, supplied by Gurit®, as a substrate. The Nylon® has been chosen as an example in this study, however, any textile fabric compatible with GO can be used as demonstrated in our earlier studies.[44] For the coating process, the pristine fabric was soaked in a GO solution. The GO, supplied in the form of aqueous paste, was obtained from Abalonyx AS, Norway. The aqueous acidic GO paste contains 25% GO, 74% water and 1–1.5% HCl by weight. The GO solution was prepared by diluting aqueous acidic GO paste of concentration about 100 mg/mL to a concentration of 2.5 mg/mL. The solution was sonicated in a bath sonicator at a frequency of 50 Hz for 30 min with the bath temperature maintained at 47°C. A sheet of the Nylon® ply was soaked in the solution for 24 h and then dried in a controlled environment at 80°C for 5 h. Once the GO was deposited on the samples, it was partially reduced by heating under the same controlled environment at 170°C for 24 h. The coating process is repeated until uniform coating throughout the fabric was achieved. The pRGO coated fabrics exhibit a smooth coating that wraps every fiber. The appearance of the coated fabrics is like that of a shiny gray fabric (see Figure 1). Under a scanning electron microscope (SEM), the coating looks very smooth, adhering well to the fibers' surface (see Figure 1).

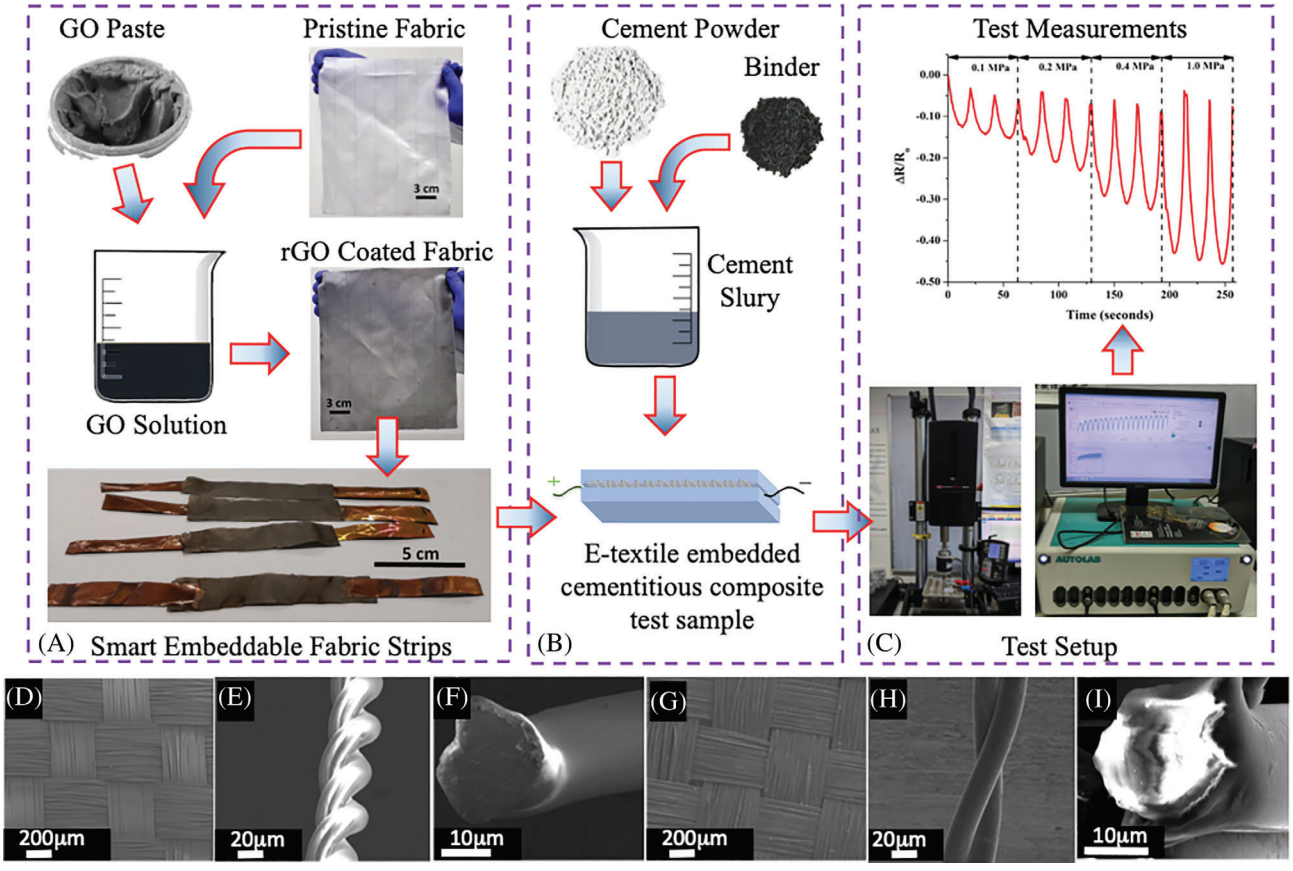

FIGURE 1 Manufacturing of e-textile embedded pure cement and polymer-modified cement structures. (A) Process for coating of Nylon® fabric with pRGO. (B) Schematic representation of manufacturing process for e-textile embedded cement structures, (C) Piezoresistive performance measurement setup testing of e-textile embedded and SEM images of (D) pure Nylon® fabric, (E) single pure Nylon® fiber, (F) cross section of a single Nylon® fiber, (G) pRGO coated Nylon® fabric, (H) pRGO coated Nylon® fibers and (I) cross section of single pRGO coated Nylon® fiber

2.2 | Compression testing sample preparation

The prepared e-textiles were subsequently embedded in plain and polymer modified cementitious matrices. For the preparation of the matrices a slurry was prepared using plain white cement obtained from a local supplier (UltraTech®). The cement was thoroughly mixed with water in a water to cement ratio of 0.67 (water to cement ration of 2:3) to form the slurry. The samples were prepared by pouring the slurry in metallic molds ($200 \times 10 \times 5$ mm) in two stages. Initially, the slurry was poured to the middle of the mold, then a small strip of the pRGO coated fabric was placed on it and subsequently the mold was filled up to the top. The resulting product was a sandwich structure. The molds were then placed in an oven at 50°C and ambient humidity (20%) to accelerate the setting of the cementitious matrix. For the polymer-modified samples, 2% by weight Sil-Poxy™ Silicone Rubber Adhesive (Smooth-On) was mixed with the cement and water. The samples were prepared in the same exact way as described above. The samples were left for 3 days for the hydration process to evolve prior to further testing. The process is shown schematically in Figures 1B and S2B.

2.3 | Compression testing

An Instron 5969 universal testing machine with a 2 kN static loading capacity, was used for the mechanical compression tests. Each sample was placed at the bottom stationary platen of the testing frame. The top section was an indenter with rectangular cross-section of 50×10 mm. Two electrical connections were taken along the shorter side of the sample by applying copper strips using silver paste (PECLO® conductive silver paint from TedPella®). A linear force profile with an increment of 10 N/s was applied to the samples to a maximum load of 1.95 kN. After reaching the target maximum load, the unloading cycle was initiated. The electrical current was recorded using an electrochemical workstation (Autolab 302 N), and the load versus deflection curve was recorded using the Instron data acquisition system. The current values were later converted to resistance using Ohm's law and subsequently fractional change in resistance was obtained. A fixed voltage of 1 V was applied and the corresponding current was recorded during loading and unloading periods. The experimental set-up is shown schematically in Figures 1C and S3.

3 | RESULTS AND DISCUSSION

3.1 | Piezoresistive response

The e-textile embedded pure and polymer-modified cementitious samples were subjected to a loading-unloading cycle at a maximum compressive stress of 3.90 MPa (1950 N). The fractional change in resistance (FCR) as a function of stress for loading and unloading regime is shown in Figure 2A. An FCR of ~35% is recorded with an application of a compressive stress of 3.90 MPa for the plain sample. For the polymer modified matrix, the FCR is ~60% for the same stress.

This is attributed to better transfer of load to the e-textile in the polymer-modified composite. The pressure sensitivity (PS) and the corresponding strain sensitivities (gauge factors) for these measurements can be estimated by the following equations[51]:

Pressure sensitivity (PS):

$$\mathrm{PS} = \frac{\mathrm{FCR}}{\text{Compressive Stress (MPa)}} \tag{1}$$

Gauge factor (GF):

$$\mathrm{GF} = \frac{\mathrm{FCR}}{\text{Compressive Strain } (\in)} \tag{2}$$

The PS, estimated using Equation (1), for a compressive strength of 3.90 MPa for the plain matrix is about 0.10 MPa^{-1} and for that of polymer-modified specimen is 0.15 MPa^{-1}. This PS is at least 25 orders of magnitude better than state-of-the-art

particulate matter reinforced smart concrete.[52] The maximum compressive strength of 3.90 MPa corresponds to a maximum compressive strain of approximately 0.03%.[53,54] Please note that there is an approximation in relation to the sensitivity to strain of the proposed materials as the utilized literature values are from similar but slightly different composite systems. The gauge factor (GF), as estimated using Equation (2), for the plain cementitious matrix is >1100, which is at least two orders of magnitude and 30 times better than best reports on self-sensing concrete based on conductive particulate matter reinforced cement-based composites.[55]

The plain cementitious sandwich structure with embedded e-textile performs better in terms of pressure and strain sensitivity than the polymer-modified one. Nonetheless, the response for the polymer-modified samples is smooth and the curve follows an elliptical locus during the loading and unloading. The corresponding behavior of the non-modified matrix possesses a relatively linear response. Cement is a material rich in minerals such as calcium silicates, aluminates, and aluminoferrites. These minerals when in contact with water they undergo a chemical reaction, known as hydration, and with the process of time they transform from a powder form to a network of solid fibrous crystals.[56] The polymer modification of the cementitious matrix impacts the evolution of this cementitious crystalline network. The viscoelastic nature of polymer chains would reduce the brittleness of the bulk structure and would increase the toughness of the bulk material. A schematic representation of the material during loading-unloading cycle is shown in Figure 2B. It is envisaged that the presence of the polymeric chains in the matrix would affect the load transfer to the fabric and hence, the piezo-resistive response.

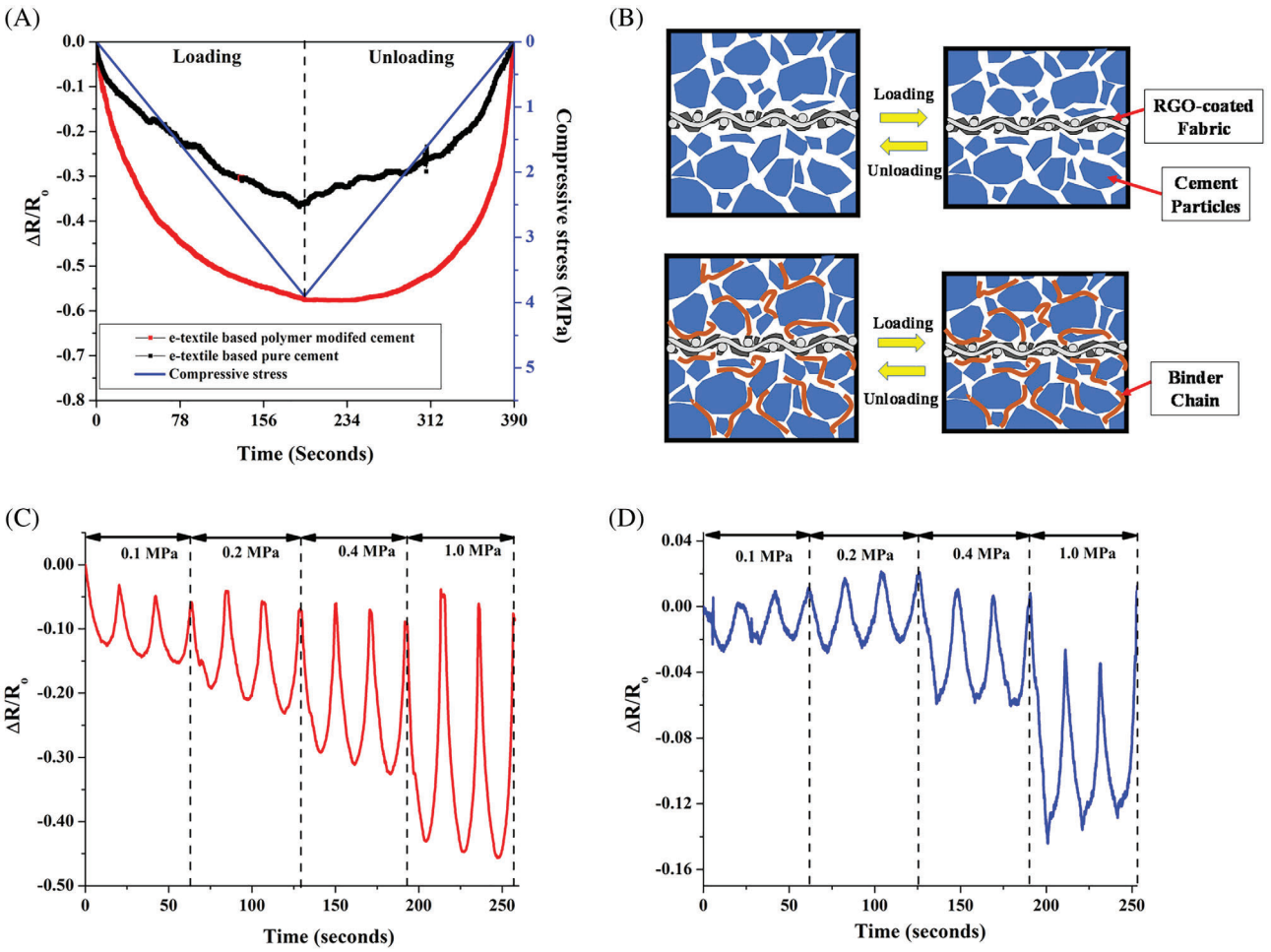

FIGURE 2 FCR response to loading and unloading of e-textile embedded pure cement and polymer-modified cement. (A) Comparison of FCR response for e-textile embedded pure cement and polymer-modified cement. (B) Schematic representation of the material during loading-unloading cycle. FCR response under various cyclic compressive loading (0.10 to 1.00 MPa): (C) e-textile embedded polymer-modified cement. (D) e-textile embedded pure cement

The FCR under various cyclic compressive loading (0.10 to 1.00 MPa) is shown in Figure 2C,D. Both plain and polymer-modified cementitious samples showed piezo-resistive response to the applied cyclic compressive stresses (0.10 to 1.00 MPa). The measurements against applied load are shown in Figure S4. The small compressive strength of 0.10 MPa causes an FCR of ∼15% corresponding to a PS of 1.50 MPa^{-1} for the polymer-modified composite. The compressive stress of 0.10 MPa in the plain cementitious matrix causes a change in resistance of ∼2% corresponding to a PS of 0.20 MPa^{-1} but a GF of ∼2000 as the strain in such low pressures for such matrix is a maximum of 0.001%. This is due to the new system of embedding the e-textile directly inside the cementitious matrix causing a maximum load transfer to the e-textile at smallest overall strain in the host matrix. To an extent the embedded textile operates like a spinal cord within the composite, sensing the stress and feeding the information to a processing unit.

The changes in resistance as a result of the applied load can be explained via two main mechanisms, namely percolation theory and quantum tunneling effect theory. When subjected to compressive strains, the number of pRGO-to-pRGO contacts increase to form more conductive paths, and the gaps between the pRGO particles decrease, leading to the manifestation of the tunneling effect, thereby causing a decrease in electrical resistance leading to the piezo-resistive phenomenon.[1,9] Also, there is variation in the shape of the peaks of FCR between plain and polymer-modified matrices highlighting possible differences in the way the electrical current is passing through the material. The FCR response as a result of applied compressive stress is shown in Figure 2A. The FCR with applied stress is about linear for the non-modified cementitious matrix and e-textile. The FCR response as a result of applied stress for the polymer-modified cementitious matrix and e-textile structure is non-linear, which could be linked to viscoelasticity of polymeric chains.

The functional durability of the sensors was tested by applying a cyclic compressive stress of 0.20 MPa for 1000 cycles as shown in Figure 3A,B. Once the electric polarization was attained, both sensors showed very good functional durability. This also validates the mechanical durability of the sensors as well as the quality of the pRGO coating on the Nylon® fabric under compression loading. The current–voltage curves of plain cement and polymer modified cement sensors under different compressive loads (from 0.00 to 1.00 MPa) are shown in Figure 3C,D. The linear current–voltage curves within the applied compressive stress range indicate that the composites obey the Ohm's law well, showing the stability of the conductive network. The resistances of the sensors in both cases are showing a decreasing trend tendency with an increase in compressive stress.

3.2 | Modeling cyclic response of piezoresistive materials

In this study, we borrowed the concept of circuit theory and employed the analogy of fault current decay to provide the analysis of the mechanisms of cyclic asymmetric resistance decay and symmetric resistance changes during long-term cyclic mechanical loading of piezoresistive materials. Unlike rated resistors, the resistance changes within the cementitious sandwich structure containing the e-fabric under cyclic mechanical loading involve transient components that cannot be ignored when dealing with the piezoresistive materials characterization. Although compared with the steady state resistance component, the transient part of the resistance change is short-lived and lasts few cycles. It needs to be included in the overall resistance change behavior of the piezoresistive materials operated under cyclic loads within a similar time frame when the transient part is still very much active.

The electrical resistance of the e-textile based composite under mechanical cyclic loading can be attributed to two major sources, that is, intrinsic resistance of the constituents, such as resistance of the cementitious matrix, polymeric binder and pRGO coated textile fabric, and contact resistance, which is the resistance between connecting pRGO flakes within the textile fabric, the resistance between pRGO and the host matrix. Some additional features such as protrusions in the fabric and its overall geometry can also affect the resistance but for the simplicity of the analysis the e-fabric was considered a single element sandwiched between the cement layers. For future analysis a detailed morphological evolution during the application of force can be carried out to understand the piezoresistive response on application of force. The intrinsic resistance of the material depends upon its ability to resist the transmittance of electrons. The intrinsic resistance of graphene depends upon its flakes' geometric parameters, their orientation and surface condition. Resistance to ionic conduction is the major source of resistance in the cement matrix while polymer is usually considered as an insulator.

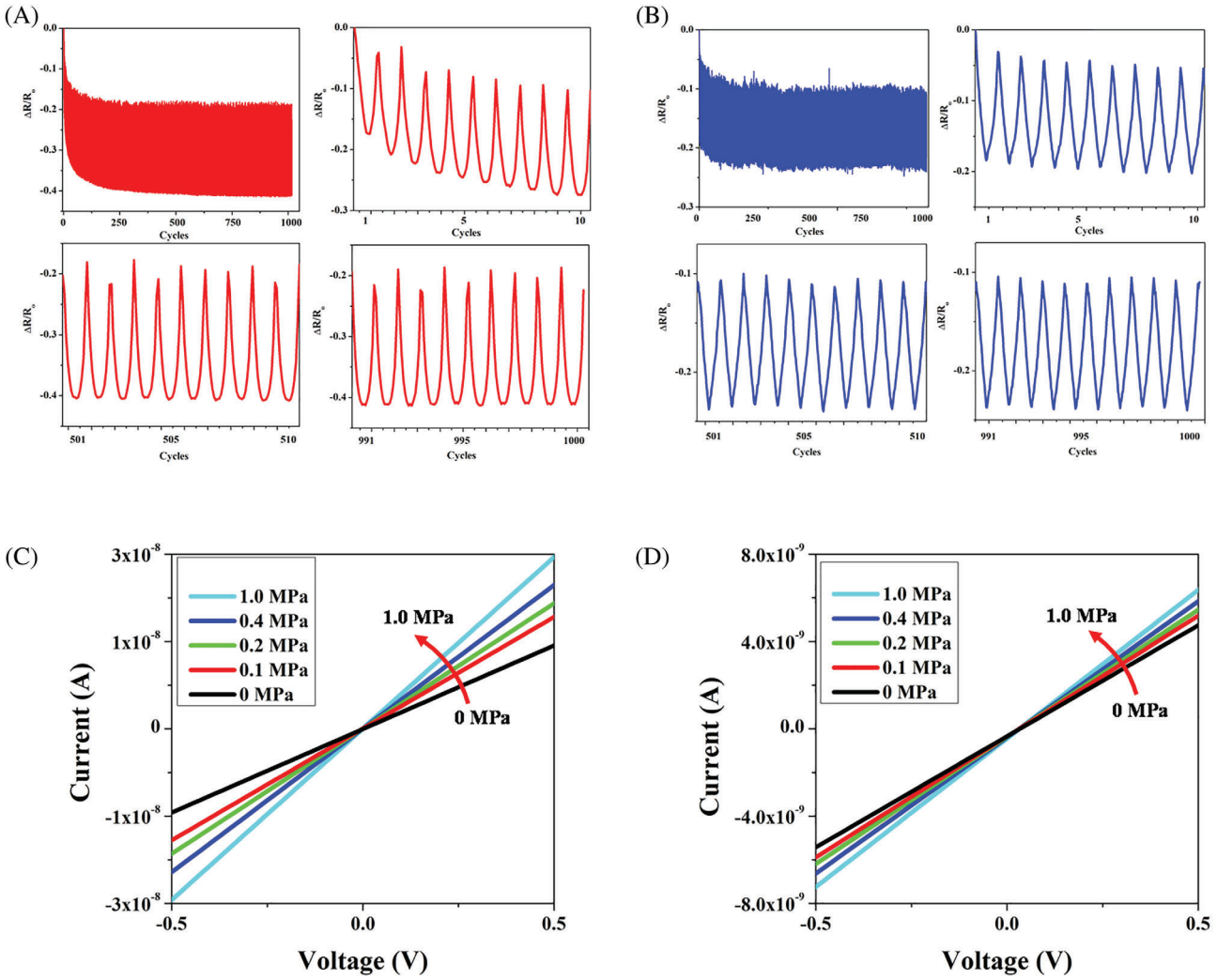

FIGURE 3 Functional durability over time for 1000 cycles at 0.20 MPa compressive stress and current–voltage (I–V) curves measured on cementitious samples with various compressive stress ranging from 0.00 to 1.00 MPa. (A) FCR response of e-textile embedded polymer modified matrix over 1000 cycles. (B) FCR response of e-textile embedded pure cementitious matrix 1000 cycles. (C) IV curves for e-textile embedded polymer modified matrix. (D) IV curves for e-textile embedded pure cementitious matrix

In this study, we assumed that the bulk resistance of the piezoresistive materials under cyclic mechanical loading is governed by intrinsic resistance of pRGO coated fabric and number of graphene flake contacts, area, their packing density, their orientation and deformation mechanisms. It was assumed that the intrinsic resistance contributes to the steady state symmetric resistance change response while the contact resistance shows transient response until it decays completely. As a result, the piezoresistive materials can be consider as higher order systems consisting of several resistors in a complex network, in which all resistor branches (conductive path) contributing to the current, Figure 4A. The transient response (resistance or current) under mechanical cyclic loading consists of multiple components, each with a different time constant. The time constant (measured in seconds) is a measure of the steepness of the transient response and it can be different for each component in a composite material system, and may depend on the individual elements' resistances, inductance as well as the frequency of the applied loading. Computing the exact component of the transient resistance will require solving set of differential equation, which is a challenging task. Moreover, if the exact components of the transient resistance are calculated, we would still need to come up preferably with a single exponential term to be able to use the concept of symmetrical based rating for piezoresistive materials.

To handle this problem, here, we used Thévenin's Theorem to simplify our complex electrical circuit to an equivalent two-terminal circuit with just a single constant voltage source in series with two resistances (or impedance)

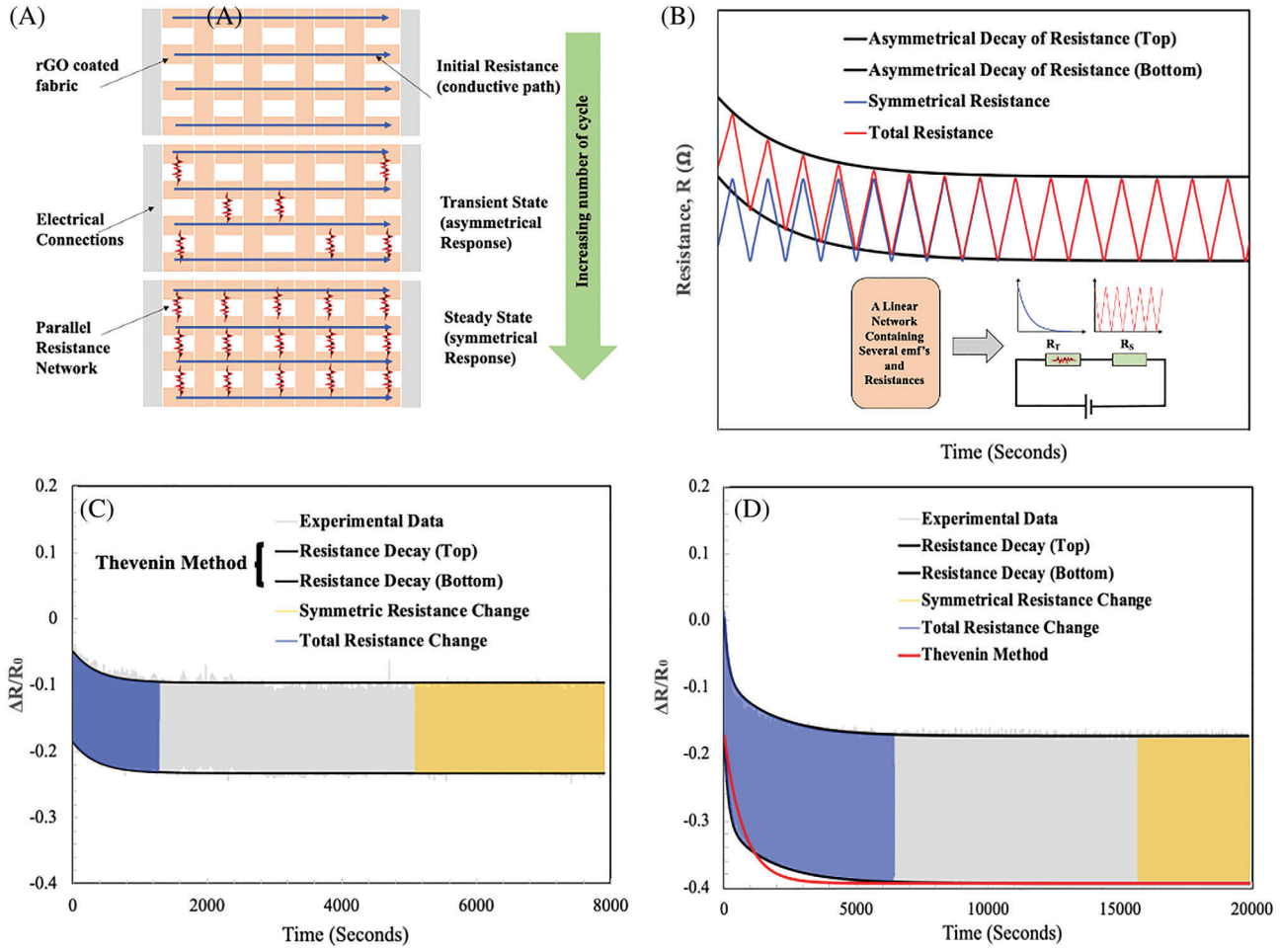

FIGURE 4 Modeling resistance change in a piezoresistive materials due to cyclic mechanical loading. (A) Schematic of the mechanism of formation of the new conductive paths during cyclic loading. (B) A simplified two resistance model representing symmetric and asymmetric part of resistance evolution during cyclic loading. (C) Modeling of change in resistance per unit original resistance for e-textile embedded pure cementitious matrix using Thevenin method (black line). (D) Modeling of change in resistance per unit original resistance for e-textile embedded polymer modified matrix using Thevenin method (red line) and higher order method (black line) with multiple decay constants

representing a transient resistance and steady state resistance change, respectively, as shown in the Figure 4B inset and can be expressed as

$$R(t) = R(t)_{\text{transient}} + R(t)_{\text{symmetric}} \tag{3}$$

Since, the time-constant is a physical characteristic of the system, so regardless of the complexity of the circuit, the transient resistance is essentially a decaying resistance can be expressed with only one time-constant following circuit reduction techniques such as Thévenin method. What naturally follows is that each material constituent branch may provide a transient resistance with the same time-constant. The transient resistance in such circuit is generally modeled as an exponentially decaying resistance and has the general form of $R_0 \exp^{(-t/\tau)}$, where R_0 is the initial resistance and τ is the decay constant. The time constant (τ) depends on the ratios of the material constants of transient to steady state resistance changes that constitutes the piezoresistive materials system under cyclic mechanical loading. Hence, when the applied cyclic load attempts to increase the number of conductive paths, the complete decay of the transient resistance is dictated by the values of material constants related to contact resistivity. The larger the parallel resistive network form, the longer it takes for the transient resistance to fade away. The general form of the total resistance change can be expressed as[57]:

$$R(t) = R_0 \left[1 - \sum_i^N R_i \left(1 - \exp^{\left(-\frac{t}{\tau_i}\right)}\right)\right] + \left[\frac{a_0}{2} + \sum_i^\infty a_n \cos(n\omega t) + \sum_i^\infty b_n \sin(n\omega t)\right] \tag{4}$$

This resistance change expression is a generalized expression to represent the decay of resistor network with multiple time decay constant subjected to any periodic cyclic loading. The first term represents the resistance decay in a piezoresistive material where multitude decay processes due to decreasing contact resistance give rise to dispersion of the decay time. Where R_0 is the initial resistance, R_i is the dimensionless material constant representing the weighted contribution of each parallel resistor branch towards the total resistance decay and τ_i represents the corresponding time constant defining steepness of the decay process.* The second term characterizes the symmetric part of the piezoresistive response due to periodic cyclic loading and can be represented by Fourier series. Where, $a_0, a_n,$ and b_n are the coefficients, and ω is the circular frequency. The a_0 is the amplitude of the symmetric steady state resistance change and can depend on amplitude of the cyclic mechanical loading for the case considered.†

Figure 4A shows the schematic of the piezoresistive material showing the initial conductive paths available within the network. With an application of the cyclic load more permanent conductive paths are produced and eventually after few cycles the steady state condition of resistance change under cyclic load is achieved as shown in Figure 4B. Equation (4) was applied assuming that both the cementitious matrix/pRGO coated fabric and cementitious matrix/polymer/pRGO coated fabric can be represented by the Thevenin's method with one decay constant. For periodic triangular cyclic loading, the parameters for symmetric resistance change are: $a_0 = A =$ Amplitude of symmetric part, $a_n = \sum_i^{\infty} \frac{-4A}{(2n-1)^2\pi^2} \cos(2n-1)\omega t$and $b_n = 0$.

For transient resistance change the parameters for cement/pRGO coated fabric are found to be $\tau_1 = 358$ s, $R_1 = 1$ while for cement/binder/pRGO coated fabric the parameters are $\tau_1 = 732$ s, $R_1 = 1$. Figure 4C,D show the comparison of the experimental data and the responses generated by the Equation (4) using Thevenin method.

For cementitious matrix/pRGO coated fabric, the Thevenin's Method found to be a good approximation, however, one time-constant is not enough to represent the resistance change response of cementitious matrix/polymer/pRGO coated fabric. It can be seen that the Thevenin's method results (shown in red color line) produce more decay than the actual decay of the piezoresistive material, so we believe that the presence of the polymeric-chains requiring more than one time constant to capture the decay response. Therefore, we used two time-constant model to capture the decay response of cement/binder/pRGO coated fabric response and found that due to the presence of the polymeric-chains in the matrix the decay of transient resistance change takes longer time. For multiple decay mechanisms in cement/binder/pRGO coated fabric the parameters are found to be $\tau_1 = 160$ s, $R_1 = 0.6$, $\tau_2 = 1750$ s, $R_2 = 0.4$. The presence of the polymeric binder produces additional time-constant due to the delayed response of the inherited viscoelastic behavior of the polymer under cyclic mechanical loading.

4 | CONCLUSION

The use of pRGO based e-textile embedded in cementitious matrices has been successfully demonstrated. It was shown that the novel e-textiles possess sensitivities as high as 1.50 MPa^{-1} and GFs as high as 2000, several orders of magnitude better than any other state-of-the-art method of self-sensing used in cement-based composites. Furthermore, the sensors showed very good mechanical stability and functional durability over long-term tests of 1000 cycles. We presented the analysis of the mechanisms of cyclic asymmetric resistance decay and symmetric resistance changes during long-term cyclic mechanical loading of piezoresistive materials. A simple relationship was developed and showed that the plain matrix resistance decay faster as compared to the polymer modified cement. For cementitious matrix/pRGO coated fabric, the Thevenin's Method found to be a good approximation of an equivalent circuit, however, non-Thevenin's calculations with at least two different decay time constants are needed to represent the resistant change response of cementitious matrix/polymer/pRGO coated fabric as a direct consequence of the viscoelastic nature of the polymeric chains.

ACKNOWLEDGMENTS

This publication is based on work supported by Abu Dhabi Award for Research Excellence (AARE-2019) under project number 8434000349 and by the Khalifa University of Science and Technology internal grants CIRA-2018-15, and FSU-2019-08. Dr Yarjan acknowledges his research visit support of Khalifa University of Science and Technology under Research Publication Award (Khan) with Project No. 8474000195. Authors have no conflict of interest relevant to this article.

AUTHOR CONTRIBUTIONS

Muhammad S Irfan: Conceptualization (equal); data curation (equal); formal analysis (equal); writing – original draft (lead); writing – review and editing (equal). **Yarjan Abdul Samad:** Conceptualization (lead); data curation (lead); formal analysis (equal); investigation (equal); supervision (lead); writing – original draft (equal); writing – review and editing (supporting).

PEER REVIEW

The peer review history for this article is available at https://publons.com/publon/10.1002/eng2.12468.

DATA AVAILABILITY STATEMENT

The data that support the findings of this study are available from the corresponding author upon reasonable request.

ENDNOTES

*It is also important to notice that the time constant of the system is solely determined by the circuit's elements resistance; no other variable such as voltage amplitude, cyclic mechanical loading amplitude and phase or the initial conditions of the circuit has any impact on the time-constant.

†While the rate of decay of the transient resistance depends only on the circuit elements, its amplitude depends on input voltage, cyclic mechanical loading circuit elements, and, importantly, on the initial conditions of the system.

ORCID

Yarjan Abdul Samad https://orcid.org/0000-0002-3432-3719

REFERENCES

1. Zhan M, Pan G, Zhou F, Mi R, Shah SP. In situ-grown carbon nanotubes enhanced cement-based materials with multifunctionality. *Cement Concrete Compos*. 2020;108:103518. doi:10.1016/j.cemconcomp.2020.103518
2. Nasibulina LI, Anoshkin IV, Nasibulin AG, Cwirzen A, Penttala V, Kauppinen EI. Effect of carbon nanotube aqueous dispersion quality on mechanical properties of cement composite. *J Nanomater*. 2012;2012:1-6.
3. Brownjohn JM. Structural health monitoring of civil infrastructure. *Philos Trans Royal Soc A Math Phys Eng Sci*. 2007;365:589-622.
4. Tseng K-H, Soh CK, Gupta A, Bhalla S. Health monitoring of civil infrastructure using smart piezoelectric transducer patches. *WIT Trans Built Environ*. 2000;46. https://www.witpress.com/elibrary/wit-transactions-on-the-built-environment/46/4726
5. Tennyson R, Mufti A, Rizkalla S, Tadros G, Benmokrane B. Structural health monitoring of innovative bridges in Canada with fiber optic sensors. *Smart Mater Struct*. 2001;10:560-573. doi:10.1088/0964-1726/10/3/320
6. Merzbacher C, Kersey AD, Friebele E. Fiber optic sensors in concrete structures: a review. *Smart Mater Struct*. 1996;5:196-208. doi:10.1088/0964-1726/5/2/008
7. Song G, Mo Y, Otero K, Gu H. Health monitoring and rehabilitation of a concrete structure using intelligent materials. *Smart Mater Struct*. 2006;15:309-314. doi:10.1088/0964-1726/15/2/010
8. Soh CK, Tseng KK, Bhalla S, Gupta A. Performance of smart piezoceramic patches in health monitoring of a RC bridge. *Smart Mater Struct*. 2000;9:533-542. doi:10.1088/0964-1726/9/4/317
9. Dong W, Li W, Tao Z, Wang K. Piezoresistive properties of cement-based sensors: review and perspective. *Construct Build Mater*. 2019;203:146-163. doi:10.1016/j.conbuildmat.2019.01.081
10. Yoo D-Y, You I, Lee S-J. Electrical properties of cement-based composites with carbon nanotubes, graphene, and graphite nanofibers. *Sensors*. 2017;17:1064. doi:10.3390/s17051064
11. Tokognon CA, Gao B, Tian GY, Yan Y. Structural health monitoring framework based on Internet of Things: a survey. *IEEE Internet Things J*. 2017;4:619-635. doi:10.1109/JIOT.2017.2664072
12. Zhang J, Tian GY, Marindra AM, Sunny AI, Zhao AB. A review of passive RFID tag antenna-based sensors and systems for structural health monitoring applications. *Sensors*. 2017;17:265.
13. Azhari F, Banthia N. Cement-based sensors with carbon fibers and carbon nanotubes for piezoresistive sensing. *Cem Concr Compos*. 2012;34:866-873.
14. Chacko RM, Banthia N, Mufti AA. Carbon-fiber-reinforced cement-based sensors. *Can J Civil Eng*. 2007;34:284-290. doi:10.1139/l06-092
15. Wen S, Chung D. Uniaxial tension in carbon fiber reinforced cement, sensed by electrical resistivity measurement in longitudinal and transverse directions. *Cem Concr Res*. 2000;30:1289-1294.
16. Rao R, Sindu B, Sasmal S. Synthesis, design and piezo-resistive characteristics of cementitious smart nanocomposites with different types of functionalised MWCNTs under long cyclic loading. *Cem Concr Compos*. 2020;108:103517.
17. García-Macías E, Downey A, D'Alessandro A, Castro-Triguero R, Laflamme S, Ubertini F. Enhanced lumped circuit model for smart nanocomposite cement-based sensors under dynamic compressive loading conditions. *Sens Actuator A Phys*. 2017;260:45-57. doi:10.1016/j.sna.2017.04.004

18. Rafiee MA, Narayanan TN, Hashim DP, et al. Hexagonal boron nitride and graphite oxide reinforced multifunctional porous cement composites. *Adv Funct Mater*. 2013;23:5624-5630.
19. Wang Y, Yang J, Ouyang D. Effect of Graphene oxide on mechanical properties of cement mortar and its strengthening mechanism. *Materials*. 2019;12:3753.
20. Wu Y-Y, Que L, Cui Z, Lambert P. Physical properties of concrete containing graphene oxide nanosheets. *Materials*. 2019;12:1707.
21. Dimov D, Amit I, Gorrie O, et al. Ultrahigh performance nanoengineered graphene–concrete composites for multifunctional applications. *Adv Funct Mater*. 2018;28:1705183. doi:10.1002/adfm.201705183
22. Hou D, Lu Z, Li X, Ma H, Li Z. Reactive molecular dynamics and experimental study of graphene-cement composites: structure, dynamics and reinforcement mechanisms. *Carbon*. 2017;115:188-208. doi:10.1016/j.carbon.2017.01.013
23. Yang H, Cui H, Tang W, Li Z, Han N, Xing F. A critical review on research progress of graphene/cement based composites. *Compos A Appl Sci Manuf*. 2017;102:273-296. doi:10.1016/j.compositesa.2017.07.019
24. Lu Z, Hou D, Meng L, Sun G, Lu C, Li Z. Mechanism of cement paste reinforced by graphene oxide/carbon nanotubes composites with enhanced mechanical properties. *RSC Adv*. 2015;5:100598-100605. doi:10.1039/C5RA18602A
25. Pan Z, He L, Qiu L, et al. Mechanical properties and microstructure of a graphene oxide–cement composite. *Cem Concr Compos*. 2015;58:140-147.
26. Konsta-Gdoutos MS, Batis G, Danoglidis PA, et al. Effect of CNT and CNF loading and count on the corrosion resistance, conductivity and mechanical properties of nanomodified OPC mortars. *Constr Build Mater*. 2017;147:48-57.
27. Liu Q, Gao R, Tam VW, Li W, Xiao J. Strain monitoring for a bending concrete beam by using piezoresistive cement-based sensors. *Constr Build Mater*. 2018;167:338-347. doi:10.1016/j.conbuildmat.2018.02.048
28. Sun S, Han B, Jiang S, et al. Nano graphite platelets-enabled piezoresistive cementitious composites for structural health monitoring. *Constr Build Mater*. 2017;136:314-328. doi:10.1016/j.conbuildmat.2017.01.006
29. Dong W, Li W, Lu N, Qu F, Vessalas K, Sheng D. Piezoresistive behaviours of cement-based sensor with carbon black subjected to various temperature and water content. *Compos B Eng*. 2019;178:107488.
30. Han B, Zhang L, Sun S, et al. Electrostatic self-assembled carbon nanotube/nano carbon black composite fillers reinforced cement-based materials with multifunctionality. *Compos A Appl Sci Manuf*. 2015;79:103-115. doi:10.1016/j.compositesa.2015.09.016
31. Xiao H, Li H, Ou J. Modeling of piezoresistivity of carbon black filled cement-based composites under multi-axial strain. *Sens Actuator A Phys*. 2010;160:87-93. doi:10.1016/j.sna.2010.04.027
32. Banthia N, Djeridane S, Pigeon M. Electrical resistivity of carbon and steel micro-fiber reinforced cements. *Cem Concr Res*. 1992;22:804-814.
33. Sun M-q, Liew RJ, Zhang M-H, Li W. Development of cement-based strain sensor for health monitoring of ultra high strength concrete. *Constr Build Mater*. 2014;65:630-637. doi:10.1016/j.conbuildmat.2014.04.105
34. Yoo D-Y, Kim S, Lee SH. Self-sensing capability of ultra-high-performance concrete containing steel fibers and carbon nanotubes under tension. *Sens Actuator A Phys*. 2018;276:125-136. doi:10.1016/j.sna.2018.04.009
35. Lan C, Xiao H, Liu M, Wang G, Ma M. Improved piezoresistivity of cement-based composites filled with aligned nickel powder. *Smart Mater Struct*. 2018;27:095003. doi:10.1088/1361-665x/aacbb1
36. Han B, Han B, Ou J. Experimental study on use of nickel powder-filled Portland cement-based composite for fabrication of piezoresistive sensors with high sensitivity. *Sens Actuator A Phys*. 2009;149:51-55.
37. Dong W, Li W, Wang K, Luo Z, Sheng D. Self-sensing capabilities of cement-based sensor with layer-distributed conductive rubber fibres. *Sens Actuator A Phys*. 2020;301:111763. doi:10.1016/j.sna.2019.111763
38. Dong W, Li W, Long G, Tao Z, Li J, Wang K. Electrical resistivity and mechanical properties of cementitious composite incorporating conductive rubber fibres. *Smart Mater Struct*. 2019;28:085013. doi:10.1088/1361-665x/ab282a
39. Zhu J, Li G, Feng C, Wang L, Zhang W. Effect of delaminated MXene (Ti3C2) on the performance of cement paste. *J Nanomater*. 2019;2019:1-8.
40. D'Alessandro A, Rallini M, Ubertini F, Materazzi AL, Kenny JM. Investigations on scalable fabrication procedures for self-sensing carbon nanotube cement-matrix composites for SHM applications. *Cem Concr Compos*. 2016;65:200-213.
41. Samad YA, Li Y, Alhassan SM, Liao K. Non-destroyable graphene cladding on a range of textile and other fibers and fiber mats. *RSC Adv*. 2014;4:16935-16938. doi:10.1039/C4RA01373E
42. Zhang H, Liu Y, Bilotti E, Peijs T. In-situ monitoring of interlaminar shear damage in carbon fibre composites. *Adv Compos Lett*. 2015;24:096369351502400405. doi:10.1177/096369351502400405
43. Zhang H, Liu Y, Kuwata M, Bilotti E, Peijs T. Improved fracture toughness and integrated damage sensing capability by spray coated CNTs on carbon fibre prepreg. *Compos A Appl Sci Manuf*. 2015;70:102-110. doi:10.1016/j.compositesa.2014.11.029
44. Ali MA, Umer R, Khan KA, Samad YA, Liao K, Cantwell W. Graphene coated piezo-resistive fabrics for liquid composite molding process monitoring. *Compos Sci Technol*. 2017;148:106-114.
45. Samad YA, Komatsu K, Yamashita D, et al. From sewing thread to sensor: nylon® fiber strain and pressure sensors. *Sens Actuator B*. 2017;240:1083-1090.
46. Butakova M, Saribekyan S, Mikhaylov A. Influence of silicon-containing additives on concrete waterproofness property. *Mater Sci Eng Conf Ser*. 2017;262:012006. doi:10.1088/1757-899x/262/1/012006
47. Qin G, Shen Z, Yu Y, Fan L, Cao H, Yin C. Effect of silicone rubber of a waste composite insulator on cement mortar properties. *Materials*. 2019;12:2796.
48. N. Makul, Modern sustainable cement and concrete composites: review of current status, challenges and guidelines, *Sustain Mater Technol*, (2020) e00155;25. doi:10.1016/j.susmat.2020.e00155

49. Pal S, Tiwari S, Katyal K, Singh A. Effect of polymer modification on structural and mechanical properties of concrete using epoxy emulsion as the modifier. *Innovation in Materials Science and Engineering*. Springer; 2019:1-10.
50. Siddika A, Al Mamun MA, Alyousef R, Amran YM, Aslani F, Alabduljabbar H. Properties and utilizations of waste tire rubber in concrete: a review. *Constr Build Mater*. 2019;224:711-731. doi:10.1016/j.conbuildmat.2019.07.108
51. Monteiro A, Loredo A, Costa P, Oeser M, Cachim P. A pressure-sensitive carbon black cement composite for traffic monitoring. *Constr Build Mater*. 2017;154:1079-1086. doi:10.1016/j.conbuildmat.2017.08.053
52. Li H, Xiao H-g, Ou J-p. A study on mechanical and pressure-sensitive properties of cement mortar with nanophase materials. *Cem Concr Res*. 2004;34:435-438. doi:10.1016/j.cemconres.2003.08.025
53. Noushini A, Aslani F, Castel A, Gilbert RI, Uy B, Foster S. Compressive stress-strain model for low-calcium fly ash-based geopolymer and heat-cured Portland cement concrete. *Cem Concr Compos*. 2016;73:136-146.
54. Li VC, Wang S, Wu C. Tensile strain-hardening behavior of polyvinyl alcohol engineered cementitious composite (PVA-ECC). *ACI Mater J Am Concr Inst*. 2001;98:483-492. https://www.concrete.org/publications/internationalconcreteabstractsportal.aspx?m=details&ID=10851
55. Saafi M, Tang L, Fung J, et al. Graphene/fly ash geopolymeric composites as self-sensing structural materials. *Smart Mater Struct*. 2014;23:065006. doi:10.1088/0964-1726/23/6/065006
56. Hewlett P, Liska M. *Lea's Chemistry of Cement and Concrete*. Butterworth-Heinemann; 2019.
57. Khan KA, Muliana A. Fully coupled heat conduction and deformation analyses of nonlinear viscoelastic composites. *Compos Struct*. 2012;94:2025-2037.

SUPPORTING INFORMATION

Additional supporting information may be found online in the Supporting Information section at the end of this article.

How to cite this article: Irfan MS, Ali MA, Khan KA, Umer R, Kanellopoulos A, Abdul Samad Y. An electronic textile embedded smart cementitious composite. *Engineering Reports*. 2021;e12468. doi: 10.1002/eng2.12468